Sciences & Technologie **B – N°22,** Décembre (2004), pp. 7-12.

STUDY OF RECTANGULAR MICROSTRIP PATCH OVER GROUND PLANE WITH RECTANGULAR APERTURE USING GALERKIN'S METHOD IN THE VECTOR FOURIER TRANSFORM DOMAIN

Received 14/07/2003 – Accepted 31/12/2004

Abstract

In this paper, a rigorous full-wave analysis of rectangular microstrip patches over ground planes with rectangular apertures in substrates containing isotropic and anisotropic materials is presented. The dyadic Green's functions of the problem are efficiently determined in the vector Fourier transform domain (VFTD). The integral equations for the unknowns patch current and aperture field are solved numerically by applying the Galerkin method of moments. The TM set of modes issued from the magnetic wall cavity model are used to expand the unknown current on the patch. Also, the same basis functions are used for approximating the aperture field in accordance with the concept of complementary electromagnetic structures. The validity of the solution is tested by comparison of computed results with experimental data. Numerical results show that changes in aperture length can drastically shift the resonant frequency. The aperture width, on the other hand, can be used for a fine adjustment of the operating frequency.

Keywords: *Patch; ground plane with aperture; anisotropy; full-wave analysis.*

Résumé

Dans cet article, une analyse rigoureuse par onde complète des plaques microbandes rectangulaires sur plans de masse avec ouvertures rectangulaires dans des substrats contenants des matériaux isotropes et anisotropes est présentée. Les fonctions tensorielles de Green du problème sont efficacement déterminées dans le domaine de la transformée vectorielle de Fourier. Les équations intégrales pour les inconnus qui sont le courant de la plaque et le champ de l'ouverture sont résolues numériquement en appliquant la méthode de Galerkin. Le groupe TM des modes issus du modèle de la cavité à mur magnétique est utilisé pour développer le courant inconnu sur la plaque. Aussi, les mêmes fonctions de base sont utilisées pour l'approximation du champ de l'ouverture en accord avec le concept des structures électromagnétiquement complémentaires. La validité de la solution est testée par comparaison des résultats calculés avec des données expérimentales. Les résultats numériques montrent que les changements dans la longueur de l'ouverture peut radicalement décaler la fréquence de résonance. La largeur de l'ouverture, d'autre part, peut être utiliser pour un ajustement fin de la fréquence d'opération.

Mots clés: *Plaque ; plan de masse avec ouverture ; anisotropie ; analyse par onde complète.*

T. FORTAKI
A. BENGHALIA
Electronics Department
University Mentouri
Constantine, Algeria

ملخص

يسعى هذا المقال إلى دراسة تحليلية عن طريق الموجة الشاملة لصفائح على شكل شرائط مدققة مستطيلة فوق مستويات أرضية تحوي فتحات مستطيلة في عوازل تظم مواد متجانسة وغير متجانسة قد قدمت. دوال جرين المصفوفية للمشكل تم تعيينها بفعالية في مجال تحويل فوري الشعاعي. حلت المعادلات التكاملية للمجاهيل المتمثلة في تيار الصفيحة وحقل الفتحة عدديا باستعمال طريقة جالركين. استعملت مجموعة الأنماط النابعة من نموذج الجوف ذو الجدار المغناطيسي من أجل نشر التيار االمجهول فوق الصفيحة. استعملت أيضا نفس الدوال القاعدية من أجل تقريب حقل الفتحة بالتلاؤم مع مفهوم التركيبات االكهرومغناطسية المتكاملة. اختبرت صحة الحل بمقارنة النتائج العددية مع المعطيات التجريبية. توضح النتائج العددية أن االتغيرات في طول الفتحة يمكن أن تؤدي إلى إزاحة جذرية لتواتر التناغم. يمكن عرض الفتحة من جهة أخرى إستعمال في تعديل طفيف لتواتر التشغيل.

الكلمات المفتاحية: *تحليلية عن طريق الموجة الشاملة، لصفائح على شكل شرائط مدققة مستطيلة، مواد غير متجانسة.*

In microstrip antenna designs, it is important to ascertain the resonant frequency of the antenna accurately because microstrip antennas have narrow bandwidths and can only operate effectively in the vicinity of the resonant frequency. As such, a theory to help ascertain the resonant frequency is helpful in antenna designs [1].

Numerous advantages have been obtained by feeding a radiating element through an aperture cut into a microstrip line ground plane [2]. Such advantages include weak parasitic radiation in the useful direction with respect to conventionally fed antennas and optimal performance for both the feeding network and antenna element. In addition, the presence of aperture on the ground plane adds new design parameters that can be used to tune the antenna impedance and resonance frequency, without modifying the radiating patch it self. A rectangular coupling aperture introduces two physical parameters-its length and width. Since the presence of apertures in the ground planes of microstrip antennas affects the resonant properties of these antennas, to develop an accurate theoretical method for predicting the aperture effect is of considerable interest. This effect of ground-plane apertures on microstrip patches has been first studied by Kawano *et al*. [3, 4]. The full-wave analysis presented in [3, 4] is unable to account for the effect of radiation damping encountered in microstrip antennas, since the considered structure was enclosed by shielding walls. The radiation damping gives rise to a complex resonant frequency, which provides the information of

© Université Mentouri, Constantine, Algérie, 2004.

the resonant frequency, the quality factor, and the half-power bandwidth of the patch antenna. Also, only patches and apertures with very narrow dimensions along the x direction are considered in the numerical procedure.

This paper presents a rigorous full-wave analysis of the rectangular microstrip antenna with a rectangular aperture in the ground plane. To the best of our knowledge, this subject has not been reported in the open literature, only full-wave analysis of circular microstrip antennas with circular apertures in the ground planes has been presented recently by Losada *et al*. [2].

Apart from microstrip antennas with apertures in the ground planes, in the last few years, there has been a growing interest in analyzing microstrip structures on anisotropic substrates [5-7]. Bearing in mind that many practical substrate materials used in microstrip antennas exhibit a significant amount of anisotropy that can affect the performance of printed antennas, and thus accurate characterization and design must account for this effect. Due to this, the present work is performed both for the case of isotropic and anisotropic dielectrics.

ANALYSIS METHOD

The problem to be solved is illustrated in Figure 1. Here we have a rectangular microstrip patch of length L_p along the x direction and width W_p along the y direction over a ground plane with a rectangular aperture of length L_a and width W_a. Both the center of the patch and the center of the aperture have the coordinate value $(x, y) = (0, 0)$.

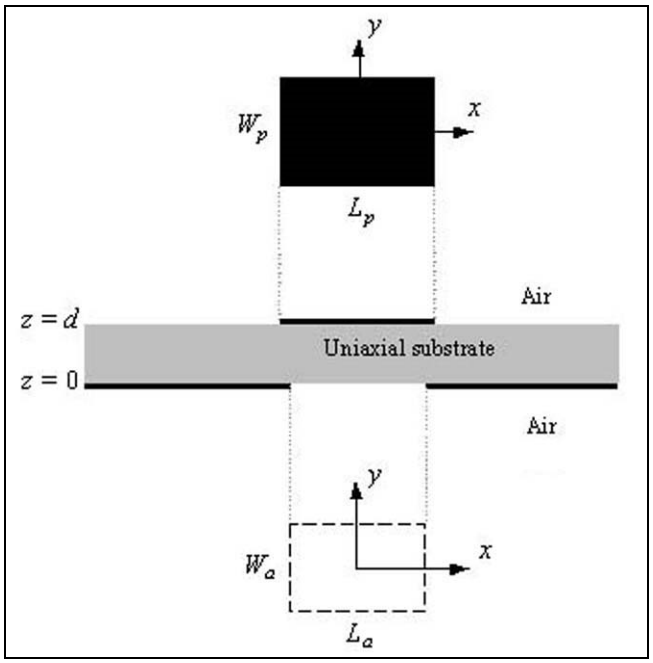

Figure 1: Geometrical structure of a rectangular microstrip patch over a ground plane with a rectangular aperture.

Also, the metallic patch and the ground plane are assumed to be perfect electric conductors of neglecting thickness. The substrate material is uniaxially anisotropic with the optical axis normal to the patch. The uniaxial substrate is characterized by the free-space permeability μ_0 and a permittivity tensor of the form

$$\bar{\varepsilon} = \varepsilon_0 \,\mathrm{diag}\left[\varepsilon_x, \varepsilon_x, \varepsilon_z\right] \tag{1}$$

ε_0 is the free-space permittivity and diag stands for the diagonal matrix with the diagonal elements appearing between the brackets. Equation (1) can be specialized to the isotropic substrate by allowing $\varepsilon_x = \varepsilon_z = \varepsilon_r$. The ambient medium is air with constitutive parameters μ_0 and ε_0. All fields and currents are time harmonic with the $e^{i\omega t}$ time dependence suppressed. The analysis needs three steps to obtain the complex resonant frequency of the rectangular microstrip antenna with a rectangular aperture in the ground plane.

Derivation of dyadic Green's functions in the VFTD

In this subsection an efficient technique to derive the dyadic Green's functions for microstrip patch over ground plane with aperture is proposed. The transverse fields inside the uniaxial anisotropic region $(0\langle z\langle d)$ can be obtained via the inverse vector Fourier transforms as [8]

$$\mathbf{E}(\mathbf{r}_s, z) = \begin{bmatrix} E_x(\mathbf{r}_s, z) \\ E_y(\mathbf{r}_s, z) \end{bmatrix} = \frac{1}{4\pi^2} \int_{-\infty}^{+\infty} \int_{-\infty}^{+\infty} \bar{\mathbf{F}}(\mathbf{k}_s, \mathbf{r}_s) \,.\, \mathbf{e}(\mathbf{k}_s, z) dk_x dk_y \tag{2}$$

$$\mathbf{H}(\mathbf{r}_s, z) = \begin{bmatrix} H_y(\mathbf{r}_s, z) \\ -H_x(\mathbf{r}_s, z) \end{bmatrix} = \frac{1}{4\pi^2} \int_{-\infty}^{+\infty} \int_{-\infty}^{+\infty} \bar{\mathbf{F}}(\mathbf{k}_s, \mathbf{r}_s) \,.\, \mathbf{h}(\mathbf{k}_s, z) dk_x dk_y \tag{3}$$

where

$$\bar{\mathbf{F}}(\mathbf{k}_s, \mathbf{r}_s) = \frac{1}{k_s} \begin{bmatrix} k_x & k_y \\ k_y & -k_x \end{bmatrix} e^{i\mathbf{k}_s \cdot \mathbf{r}_s}, \quad \mathbf{r}_s = \hat{\mathbf{x}}\, x + \hat{\mathbf{y}}\, y,$$

$$\mathbf{k}_s = \hat{\mathbf{x}}\, k_x + \hat{\mathbf{y}}\, k_y, \quad k_s = |\mathbf{k}_s|$$

$$\mathbf{e}(\mathbf{k}_s, z) = e^{-i\bar{\mathbf{k}}_z z} \cdot \mathbf{A}(\mathbf{k}_s) + e^{i\bar{\mathbf{k}}_z z} \cdot \mathbf{B}(\mathbf{k}_s) \tag{4}$$

$$\mathbf{h}(\mathbf{k}_s, z) = \bar{\mathbf{g}}(\mathbf{k}_s) \cdot \left[e^{-i\bar{\mathbf{k}}_z z} \cdot \mathbf{A}(\mathbf{k}_s) - e^{i\bar{\mathbf{k}}_z z} \cdot \mathbf{B}(\mathbf{k}_s) \right] \tag{5}$$

In (4) and (5), **A** and **B** are two-component unknown vectors and

$$\bar{\mathbf{k}}_z = \mathrm{diag}\left[k_z^e, k_z^h\right], \bar{\mathbf{g}}(\mathbf{k}_s) = \mathrm{diag}\left[\frac{\omega \varepsilon_0 \varepsilon_x}{k_z^e}, \frac{k_z^h}{\omega \mu_0}\right] \tag{6}$$

k_z^e and k_z^h are, respectively, propagation constants for TM and TE waves in the uniaxial substrate [6]. Writing (4) and (5) in the plane $z = 0$ and $z = d$, and by eliminating the unknowns **A** and **B**, we obtain the matrix form

$$\begin{bmatrix} \mathbf{e}(\mathbf{k}_s, d^-) \\ \mathbf{h}(\mathbf{k}_s, d^-) \end{bmatrix} = \bar{\mathrm{T}} \cdot \begin{bmatrix} \mathbf{e}(\mathbf{k}_s, 0^+) \\ \mathbf{h}(\mathbf{k}_s, 0^+) \end{bmatrix} \tag{7}$$

with

$$\bar{\mathbf{T}} = \begin{bmatrix} \bar{\mathbf{T}}^{11} & \bar{\mathbf{T}}^{12} \\ \bar{\mathbf{T}}^{21} & \bar{\mathbf{T}}^{22} \end{bmatrix} = \begin{bmatrix} \cos\bar{\boldsymbol{\theta}} & -i\,\bar{\mathbf{g}}^{-1} \cdot \sin\bar{\boldsymbol{\theta}} \\ -i\bar{\mathbf{g}} \cdot \sin\bar{\boldsymbol{\theta}} & \cos\bar{\boldsymbol{\theta}} \end{bmatrix}, \bar{\boldsymbol{\theta}} = \bar{\mathbf{k}}_z d \tag{8}$$

which combines **e** and **h** on both sides of the uniaxial anisotropic region as input and output quantities. The continuity equations for the tangential field components at the interface $z = d$ are

$$\mathbf{e}(\mathbf{k}_s, d^-) = \mathbf{e}(\mathbf{k}_s, d^+) = \mathbf{e}(\mathbf{k}_s, d) \tag{9}$$

$$\mathbf{h}(\mathbf{k}_s, d^-) - \mathbf{h}(\mathbf{k}_s, d^+) = \mathbf{j}(\mathbf{k}_s) \tag{10}$$

$\mathbf{j}(\mathbf{k}_s)$ in (10) is related to the vector Fourier transform of $\mathbf{J}(\mathbf{r}_s)$, the current on the patch, as [9]

$$\mathbf{j}(\mathbf{k}_s) = \int_{-\infty}^{+\infty}\int_{-\infty}^{+\infty} \bar{\mathbf{F}}(\mathbf{k}_s, -\mathbf{r}_s).\mathbf{J}(\mathbf{r}_s) dk_x dk_y, \ \mathbf{J}(\mathbf{r}_s) = \begin{bmatrix} J_x(\mathbf{r}_s) \\ J_y(\mathbf{r}_s) \end{bmatrix} \tag{11}$$

The continuity equations for the tangential field components at the interface $z = 0$ are

$$\mathbf{e}(\mathbf{k}_s, 0^-) = \mathbf{e}(\mathbf{k}_s, 0^+) = \mathbf{e}(\mathbf{k}_s, 0) \tag{12}$$

$$\mathbf{h}(\mathbf{k}_s, 0^-) - \mathbf{h}(\mathbf{k}_s, 0^+) = \mathbf{j}_0(\mathbf{k}_s) \tag{13}$$

In (13), $\mathbf{j}_0(\mathbf{k}_s)$ is the vector Fourier transform of the current $\mathbf{J}_0(\mathbf{r}_s)$ on the ground plane with a rectangular aperture. In the unbounded air region above the patch (below the aperture) the electromagnetic field given by (4) and (5) should vanish at $z \to +\infty$ ($z \to -\infty$) according to Sommerfeld's condition of radiation, this yields

$$\mathbf{h}(\mathbf{k}_s, d^+) = \bar{\mathbf{g}}_0(\mathbf{k}_s) \cdot \mathbf{e}(\mathbf{k}_s, d^+) \tag{14}$$

$$\mathbf{h}(\mathbf{k}_s, 0^-) = -\bar{\mathbf{g}}_0(\mathbf{k}_s) \cdot \mathbf{e}(\mathbf{k}_s, 0^-) \tag{15}$$

where $\bar{\mathbf{g}}_0(\mathbf{k}_s)$ can be easily obtained from the expression of $\bar{\mathbf{g}}(\mathbf{k}_s)$ given in (6) by allowing $\varepsilon_x = \varepsilon_z = \varepsilon_r = 1$. Combining (7), (9), (10), and (12)-(15), we obtain a relation among $\mathbf{j}(\mathbf{k}_s)$, $\mathbf{j}_0(\mathbf{k}_s)$, $\mathbf{e}(\mathbf{k}_s, d)$, and $\mathbf{e}(\mathbf{k}_s, 0)$ given by

$$\mathbf{e}(\mathbf{k}_s, d) = \bar{\mathbf{G}}(\mathbf{k}_s).\mathbf{j}(\mathbf{k}_s) + \bar{\mathbf{\Psi}}(\mathbf{k}_s).\mathbf{e}(\mathbf{k}_s, 0) \tag{16}$$

$$\mathbf{j}_0(\mathbf{k}_s) = -\bar{\mathbf{\Phi}}(\mathbf{k}_s).\mathbf{j}(\mathbf{k}_s) - \bar{\mathbf{Y}}(\mathbf{k}_s).\mathbf{e}(\mathbf{k}_s, 0) \tag{17}$$

where

$$\bar{\mathbf{G}}(\mathbf{k}_s) = \mathrm{diag}\left[G^e, G^h\right] = \left[\bar{\mathbf{T}}^{22}.\left(\bar{\mathbf{T}}^{12}\right)^{-1} - \bar{\mathbf{g}}_0\right]^{-1} \tag{18}$$

$$\bar{\mathbf{\Psi}}(\mathbf{k}_s) = \mathrm{diag}\left[\Psi^e, \Psi^h\right] = \bar{\mathbf{\Phi}}(\mathbf{k}_s)$$

$$= \mathrm{diag}\left[\Phi^e, \Phi^h\right] = \left(\bar{\mathbf{T}}^{12}\right)^{-1}.\bar{\mathbf{G}}(\mathbf{k}_s) \tag{19}$$

$$\bar{\mathbf{Y}}(\mathbf{k}_s) = \mathrm{diag}\left[Y^e, Y^h\right] = \bar{\mathbf{g}}_0 - \bar{\mathbf{\Psi}}(\mathbf{k}_s).\left[\bar{\mathbf{T}}^{21} - \bar{\mathbf{g}}_0 \ . \ \bar{\mathbf{T}}^{11}\right]$$

The four 2x2 diagonal matrices $\bar{\mathbf{G}}(\mathbf{k}_s)$, $\bar{\mathbf{\Psi}}(\mathbf{k}_s)$, $\bar{\mathbf{\Phi}}(\mathbf{k}_s)$, and $\bar{\mathbf{Y}}(\mathbf{k}_s)$ stand for a set of dyadic Green's functions in the VFTD. It is to be noted that $\bar{\mathbf{G}}(\mathbf{k}_s)$ is related to the patch current and $\bar{\mathbf{Y}}(\mathbf{k}_s)$ is related to the aperture field. $\bar{\mathbf{\Psi}}(\mathbf{k}_s)$, and $\bar{\mathbf{\Phi}}(\mathbf{k}_s)$ represent the interactions between the patch current and aperture field. In (16) and (17) the unknowns are $\mathbf{j}(\mathbf{k}_s)$ and $\mathbf{e}(\mathbf{k}_s, 0)$. Another possible choice in the analysis of microstrip patches over ground planes with apertures is to consider $\mathbf{j}_0(\mathbf{k}_s)$ as unknown instead of $\mathbf{e}(\mathbf{k}_s, 0)$. It is anticipated, however, that a very large number of terms of basis functions would be needed for the expansion of the current $\mathbf{J}_0(\mathbf{r}_s)$ on the ground plane with aperture because of the wide conductor area. Hence, it is better to apply the Galerkin procedure to the unknown $\mathbf{E}(\mathbf{r}_s, 0)$ field at the aperture. The same reasoning has been applied in the analysis of finlines [10].

Integral equations formulation

The transverse electric field at the plane of the patch and the surface current density on the ground plane with a rectangular aperture can be obtained from (16) and (17), respectively, via the inverse vector Fourier transforms as

$$\mathbf{E}(\mathbf{r}_s, d) = \frac{1}{4\pi^2}\int_{-\infty}^{+\infty}\int_{-\infty}^{+\infty} \bar{\mathbf{F}}(\mathbf{k}_s, \mathbf{r}_s) \times$$

$$\times\left[\bar{\mathbf{G}}(\mathbf{k}_s).\mathbf{j}(\mathbf{k}_s) + \bar{\mathbf{\Psi}}(\mathbf{k}_s).\mathbf{e}(\mathbf{k}_s, 0)\right] dk_x dk_y \tag{21}$$

$$\mathbf{J}_0(\mathbf{r}_s) = -\frac{1}{4\pi^2}\int_{-\infty}^{+\infty}\int_{-\infty}^{+\infty} \bar{\mathbf{F}}(\mathbf{k}_s, \mathbf{r}_s) \times$$

$$\times\left[\bar{\Phi}(\mathbf{k}_s).\ \mathbf{j}(\mathbf{k}_s) + \bar{\mathbf{Y}}(\mathbf{k}_s).\mathbf{e}(\mathbf{k}_s, 0)\right] dk_x dk_y \tag{22}$$

Boundary conditions require that the transverse electric field of (21) vanishes on the perfectly conducting patch and the current of (22) vanishes off the ground plane, to give the following coupled integral equations for the patch current and aperture field:

$$\int_{-\infty}^{+\infty}\int_{-\infty}^{+\infty} \bar{\mathbf{F}}(\mathbf{k}_s, \mathbf{r}_s).\left[\bar{\mathbf{G}}(\mathbf{k}_s).\mathbf{j}(\mathbf{k}_s) + \bar{\mathbf{\Psi}}(\mathbf{k}_s).\mathbf{e}(\mathbf{k}_s, 0)\right] dk_x dk_y = \mathbf{0}$$

$\mathbf{r}_s \in$ patch (23)

$$\int_{-\infty}^{+\infty}\int_{-\infty}^{+\infty} \bar{\mathbf{F}}(\mathbf{k}_s, \mathbf{r}_s).\left[\bar{\mathbf{\Phi}}(\mathbf{k}_s).\mathbf{j}(\mathbf{k}_s) + \bar{\mathbf{Y}}(\mathbf{k}_s).\mathbf{e}(\mathbf{k}_s, 0)\right] dk_x dk_y = \mathbf{0}$$

$\mathbf{r}_s \in$ aperture (24)

Galerkin's method solution of the integral equations

The first step in the moment method solution of (23) and (24) is to expand both the patch current $\mathbf{J}(\mathbf{r}_s)$ and aperture field $\mathbf{E}(\mathbf{r}_s, 0)$ as

$$\mathbf{J}(\mathbf{r}_s) = \sum_{n=1}^{N} a_n \begin{bmatrix} J_{xn}(\mathbf{r}_s) \\ 0 \end{bmatrix} + \sum_{m=1}^{M} b_m \begin{bmatrix} 0 \\ J_{ym}(\mathbf{r}_s) \end{bmatrix} \tag{25}$$

$$\mathbf{E}(\mathbf{r}_s, 0) = \sum_{p=1}^{P} c_p \begin{bmatrix} E_{xp}(\mathbf{r}_s) \\ 0 \end{bmatrix} + \sum_{q=1}^{Q} d_q \begin{bmatrix} 0 \\ E_{yq}(\mathbf{r}_s) \end{bmatrix} \tag{26}$$

where J_{xn}, J_{ym}, E_{xp}, and E_{yq} are known basis functions and a_n, b_m, c_p, and d_q are the mode expansion coefficients to be sought. Using the technique known as the moment method [11], with weighting modes chosen identical to the expansion modes, (23) and (24) are reduced

to a system of linear equations which can be written compactly in matrix form as

$$\begin{bmatrix} \begin{bmatrix} (\bar{\mathbf{U}}^{11})_{N\times N} & (\bar{\mathbf{U}}^{12})_{N\times M} \\ (\bar{\mathbf{U}}^{21})_{M\times N} & (\bar{\mathbf{U}}^{22})_{M\times M} \end{bmatrix} & \begin{bmatrix} (\bar{\mathbf{V}}^{11})_{N\times P} & (\bar{\mathbf{V}}^{12})_{N\times Q} \\ (\bar{\mathbf{V}}^{21})_{M\times P} & (\bar{\mathbf{V}}^{22})_{M\times Q} \end{bmatrix} \\ \begin{bmatrix} (\bar{\mathbf{W}}^{11})_{P\times N} & (\bar{\mathbf{W}}^{12})_{P\times M} \\ (\bar{\mathbf{W}}^{21})_{Q\times N} & (\bar{\mathbf{W}}^{22})_{Q\times M} \end{bmatrix} & \begin{bmatrix} (\bar{\mathbf{Z}}^{11})_{P\times P} & (\bar{\mathbf{Z}}^{12})_{P\times Q} \\ (\bar{\mathbf{Z}}^{21})_{Q\times P} & (\bar{\mathbf{Z}}^{22})_{Q\times Q} \end{bmatrix} \end{bmatrix} \cdot \begin{bmatrix} (\mathbf{a})_{N\times 1} \\ (\mathbf{b})_{M\times 1} \\ (\mathbf{c})_{P\times 1} \\ (\mathbf{d})_{Q\times 1} \end{bmatrix} = \mathbf{0} \tag{27}$$

The elements of the matrix $(\bar{\mathbf{U}})_{(N+M)\times(N+M)}$ are given by

$$(\bar{\mathbf{U}}^{11})_{k\,n} = \int_{-\infty}^{+\infty}\int_{-\infty}^{+\infty} \frac{1}{k_s^2}[k_x^2 G^e + k_y^2 G^h]\,\tilde{J}_{x\,k}(-\mathbf{k}_s)\tilde{J}_{x\,n}(\mathbf{k}_s)\,dk_x dk_y \tag{28a}$$

$$(\bar{\mathbf{U}}^{12})_{k\,m} = \int_{-\infty}^{+\infty}\int_{-\infty}^{+\infty} \frac{k_x k_y}{k_s^2}[G^e - G^h]\,\tilde{J}_{x\,k}(-\mathbf{k}_s)\tilde{J}_{y\,m}(\mathbf{k}_s)dk_x dk_y \tag{28b}$$

$$(\bar{\mathbf{U}}^{21})_{l\,n} = \int_{-\infty}^{+\infty}\int_{-\infty}^{+\infty} \frac{k_x k_y}{k_s^2}[G^e - G^h]\,\tilde{J}_{y\,l}(-\mathbf{k}_s)\tilde{J}_{x\,n}(\mathbf{k}_s)dk_x dk_y \tag{28c}$$

$$(\bar{\mathbf{U}}^{22})_{l\,m} = \int_{-\infty}^{+\infty}\int_{-\infty}^{+\infty} \frac{1}{k_s^2}[k_y^2 G^e + k_x^2 G^h]\,\tilde{J}_{y\,l}(-\mathbf{k}_s)\tilde{J}_{y\,m}(\mathbf{k}_s)dk_x dk_y \tag{28d}$$

In (28a)-(28d), $\tilde{J}_{xn}$ and $\tilde{J}_{ym}$ are the scalar Fourier transforms of J_{xn} and J_{ym}, respectively. About the elements of the matrix $(\bar{\mathbf{V}})_{(N+M)\times(P+Q)}$ they are given by

$$(\bar{\mathbf{V}}^{11})_{k\,p} = \int_{-\infty}^{+\infty}\int_{-\infty}^{+\infty} \frac{1}{k_s^2}[k_x^2 \Psi^e + k_y^2 \Psi^h]\,\tilde{J}_{x\,k}(-\mathbf{k}_s)\tilde{E}_{x\,p}(\mathbf{k}_s)dk_x dk_y \tag{29a}$$

$$(\bar{\mathbf{V}}^{12})_{k\,q} = \int_{-\infty}^{+\infty}\int_{-\infty}^{+\infty} \frac{k_x k_y}{k_s^2}[\Psi^e - \Psi^h]\,\tilde{J}_{x\,k}(-\mathbf{k}_s)\tilde{E}_{y\,q}(\mathbf{k}_s)dk_x dk_y \tag{29b}$$

$$(\bar{\mathbf{V}}^{21})_{l\,p} = \int_{-\infty}^{+\infty}\int_{-\infty}^{+\infty} \frac{k_x k_y}{k_s^2}[\Psi^e - \Psi^h]\,\tilde{J}_{y\,l}(-\mathbf{k}_s)\tilde{E}_{x\,p}(\mathbf{k}_s)dk_x dk_y \tag{29c}$$

$$(\bar{\mathbf{V}}^{22})_{lq} = \int_{-\infty}^{+\infty}\int_{-\infty}^{+\infty} \frac{1}{k_s^2}[k_y^2 \Psi^e + k_x^2 \Psi^h]\,\tilde{J}_{yl}(-\mathbf{k}_s)\tilde{E}_{yq}(\mathbf{k}_s)dk_x dk_y \tag{29d}$$

In (29a)-(29d), $\tilde{E}_{xp}$ and $\tilde{E}_{yq}$ are the scalar Fourier transforms of E_{xp} and E_{yq}, respectively. About the elements of the matrix $(\bar{\mathbf{W}})_{(P+Q)\times(N+M)}$, they are given by

$$(\bar{\mathbf{W}}^{11})_{k`n} = \int_{-\infty}^{+\infty}\int_{-\infty}^{+\infty} \frac{1}{k_s^2}[k_x^2 \Phi^e + k_y^2 \Phi^h]\,\tilde{E}_{x\,k`}(-\mathbf{k}_s)\,\tilde{J}_{xn}(\mathbf{k}_s)dk_x dk_y \tag{30a}$$

$$(\bar{\mathbf{W}}^{12})_{k`m} = \int_{-\infty}^{+\infty}\int_{-\infty}^{+\infty} \frac{k_x k_y}{k_s^2}[\Phi^e - \Phi^h]\,\tilde{E}_{x\,k`}(-\mathbf{k}_s)\tilde{J}_{ym}(\mathbf{k}_s)dk_x dk_y \tag{30b}$$

$$(\bar{\mathbf{W}}^{21})_{l`n} = \int_{-\infty}^{+\infty}\int_{-\infty}^{+\infty} \frac{k_x k_y}{k_s^2}[\Phi^e - \Phi^h]\,\tilde{E}_{y\,l`}(-\mathbf{k}_s)\tilde{J}_{xn}(\mathbf{k}_s)dk_x dk_y \tag{30c}$$

$$(\bar{\mathbf{W}}^{22})_{l`m} = \int_{-\infty}^{+\infty}\int_{-\infty}^{+\infty} \frac{1}{k_s^2}[k_y^2 \Phi^e + k_x^2 \Phi^h]\,\tilde{E}_{y\,l`}(-\mathbf{k}_s)\tilde{J}_{ym}(\mathbf{k}_s)dk_x dk_y \tag{30d}$$

Finally the elements of the matrix $(\bar{\mathbf{Z}})_{(P+Q)\times(P+Q)}$ are given by

$$(\bar{\mathbf{Z}}^{11})_{k`p} = \int_{-\infty}^{+\infty}\int_{-\infty}^{+\infty} \frac{1}{k_s^2}[k_x^2 Y^e + k_y^2 Y^h]\,\tilde{E}_{xk`}(-\mathbf{k}_s)\tilde{E}_{xp}(\mathbf{k}_s)dk_x dk_y \tag{31a}$$

$$(\bar{\mathbf{Z}}^{12})_{k`q} = \int_{-\infty}^{+\infty}\int_{-\infty}^{+\infty} \frac{k_x k_y}{k_s^2}[Y^e - Y^h]\,\tilde{E}_{xk`}(-\mathbf{k}_s)\tilde{E}_{yq}(\mathbf{k}_s)dk_x dk_y \tag{31b}$$

$$(\bar{\mathbf{Z}}^{21})_{l`p} = \int_{-\infty}^{+\infty}\int_{-\infty}^{+\infty} \frac{k_x k_y}{k_s^2}[Y^e - Y^h]\,\tilde{E}_{yl`}(-\mathbf{k}_s)\tilde{E}_{xp}(\mathbf{k}_s)dk_x dk_y \tag{31c}$$

$$(\bar{\mathbf{Z}}^{22})_{l`q} = \int_{-\infty}^{+\infty}\int_{-\infty}^{+\infty} \frac{1}{k_s^2}[k_y^2 Y^e + k_x^2 Y^h]\,\tilde{E}_{yl`}(-\mathbf{k}_s)\tilde{E}_{yq}(\mathbf{k}_s)dk_x dk_y \tag{31d}$$

It is easy to show that the entire matrix in (27) is a symmetric matrix. For the existence of nontrivial solution of (27), we must have

$$\det(\bar{\mathbf{\Omega}}(f)) = 0\,,\quad \bar{\Omega} = \begin{bmatrix} \bar{\mathbf{U}} & \bar{\mathbf{V}} \\ \bar{\mathbf{W}} & \bar{\mathbf{Z}} \end{bmatrix} \tag{32}$$

which is only satisfied by a complex frequency $f = f_r + \mathbf{i}\,f_i$ that gives the resonant frequency f_r and the half-power bandwidth $2f_i/f_r$ of the rectangular microstrip antenna with a rectangular aperture in the ground plane.

NUMERICAL RESULTS AND DISCUSSION

Convergence and comparison of numerical results

Although the full-wave analysis can give results for several resonant modes [2, 12], only results for the TM_{01} mode are presented in this study. In applying Galerkin's method to solve the integral equations, it is advantageous to express the unknown patch current in terms of appropriate basis functions formed by the set of transverse magnetic modes of a rectangular cavity with magnetic side walls and electric top and bottom walls [13, eqs. (7a) and (7b)], and whose Fourier transforms are obtained in closed form [14, eqs. (27) and (31)]. Also, the same basis functions are used for approximating the transverse electric field on the

aperture in accordance with the concept of complementary electromagnetic structures [2, 15]. Through numerical convergence checks it is found that for small aperture, only a few number of basis functions suffices to obtain good convergence, while for wide aperture, especially when the size of the aperture is comparable to that of the patch, additional basis functions should also be included both In the approximation of the current patch and the transverse electric field on the aperture.

In order to confirm the computation accuracy, our numerical results are compared with experimental data previously published [16]. Experimental and numerical evaluations have been done with a patch of dimension 3.4 cm x 3 cm printed on isotropic substrates with a relative permittivity of 2.62. Table 1 summarizes measured and computed resonant frequencies for two different aperture sizes. Differences between numerical and experimental results are less than 1%. As a consequence, excellent agreement between theory and experiment is achieved. Note that the measured resonant frequencies in table 1 are obtained from the curves of the measured input impedance [16, figs. 4 and 5].

Table 1: Comparison of measured and calculated resonant frequencies of a rectangular microstrip antenna with a rectangular aperture in the ground plane;
$L_p \times W_p = 3.4\text{cm} \times 3\text{cm}, \varepsilon_r = 2.62$.

Aperture dimension L_a (mm) x W_a (mm)	Substrate thickness d (mm)	Resonant frequencies f_r (GHz)		Error (%)
		Measured [16]	Calculated	
7 x 0.7	0.794	2.896	2.900	0.14
10 x 1	3.175	2.750	2.770	0.73

Effect of the presence of a rectangular aperture on the resonant frequency

Figure 2 presents numerical results for the resonant frequencies of rectangular microstrip patches over ground planes with and without rectangular apertures. Note that, for the microstrip antennas without apertures, our numerical calculations agree well with the results obtained from the curve-fitting formula in [9]. It is found that the resonant frequencies of the patches over ground planes without apertures are larger than those obtained with apertures. It can also be seen that the apertures with length $L_a = 0.5W_p$ have a stronger effect on the resonant frequency than the apertures with length $L_a = 0.25W_p$. Thus, the differences between the results obtained for the resonant frequencies when $L_a = 0$ and those obtained when $L_a = 0.25W_p$ reach 3.89% for the aperture $L_a \times W_a = 0.25W_p \times 0.25W_p$ and 4.68% for the aperture $L_a \times W_a = 0.25W_p \times 0.5W_p$. However, the differences between the results obtained for the resonant frequencies when $L_a = 0$ and those obtained when $L_a = 0.5W_p$ are much larger and reach 12.85% for the aperture $L_a \times W_a = 0.5W_p \times 0.25W_p$ and 13.77% for the aperture $L_a \times W_a = 0.5W_p \times 0.5W_p$. We conclude that the aperture length has a stronger effect on the resonant frequency than the aperture width. Note also that, for a fixed aperture length, the change of the aperture width from $0.25W_p$ to $0.5W_p$ shifts slightly the resonant frequency. As an example, for the antenna having a patch width $W_p = 20\text{mm}$ and aperture of dimension $0.5W_p \times 0.25W_p$, the resonant frequency is 4.061 GHz. When the aperture width is changed from $0.25W_p$ to $0.5W_p$ and the aperture length remains constant, the resonant frequency decreases from 4.061 to 4.018 GHz for a small shift of 0.043 GHz. Therefore, the aperture width can be used for a fine adjustment of the operating frequency.

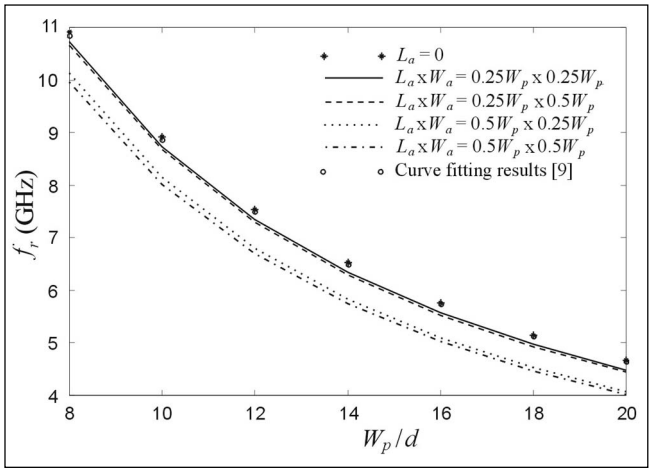

Figure 2: Resonant frequencies of rectangular microstrip patches printed on an isotropic substrate over ground planes with and without rectangular apertures;
$d = 1\text{mm}, \varepsilon_r = 2.35, L_p = 1.5W_p$.

Effect of uniaxial anisotropy in the substrate

In Table 2, results are presented for the resonant frequencies of rectangular microstrip patch over ground planes with and without rectangular apertures in the case where the patch is printed on an anisotropic dielectric substrate, i.e., Epsilam-10. The patch dimension is 1.5 cm x 1 cm and the substrate has a thickness of 1 mm.

Table 2: Resonant frequencies of rectangular microstrip patch printed on anisotropic Epsilam-10 over ground planes with and without rectangular apertures;
$d = 1\text{mm}, L_p \times W_p = 1.5\text{cm} \times 1\text{cm}$.

Aperture dimension L_a x W_a	Resonant frequencies f_r (GHz)		Fractional change (%)
	Considering anisotropy (ε_x, ε_z) = (13,10.3)	Neglecting anisotropy (ε_x, ε_z) = (10.3,10.3)	
0	4.410	4.457	1.07
$0.25L_p$ x $0.25W_p$	4.184	4.227	1.03
$0.5L_p$ x $0.5W_p$	3.564	3.608	1.23
$0.75L_p$ x $0.75W_p$	3.054	3.109	1.80
L_p x W_p	2.833	2.955	4.31

In this table, the results obtained for the patch printed on anisotropic Epsilam-10 are compared with the results that would be obtained if the anisotropy of Epsilam-10 were neglected. In the case where $L_a \times W_a = L_p \times W_p$, the difference between the results obtained considering anisotropy and neglecting anisotropy is 4.31%. However, in the other considered cases these differences are much smaller, the maximum change being 1.8% when $L_a \times W_a = 0.75L_p \times 0.75W_p$. Therefore, dielectric anisotropy effect is especially significant when the size of the aperture is similar to that of the patch. This result agrees with that discovered theoretically for circular microstrip antenna with circular aperture in the ground plane [2].

CONCLUSIONS

We have presented a rigorous full-wave analysis of rectangular microstrip patches over ground planes with rectangular apertures in substrates containing isotropic and anisotropic materials. The problem has been formulated in terms of integral equations using vector Fourier transforms. An efficient technique has been proposed for determining the dyadic Green's functions in the VFTD. Galerkin's method has been used to solve for the surface current density on the rectangular patch and the transverse electric field at the aperture. Although a single-layer microstrip antenna has been treated in this paper, it is quite straightforward to extend the analysis presented here to structures involving stratified substrates. The calculated results have been compared with measurements and excellent agreement has been found. Numerical results show that changes in aperture length can drastically shift the resonant frequency. The aperture width, on the other hand, can be used for a fine adjustment of the operating frequency. Other results also indicate that dielectric anisotropy effect is especially significant when the size of the aperture is similar to that of the patch. This last results agrees with that discovered theoretically for circular microstrip patches over ground planes with circular apertures [2].

REFERENCES

[1]- Losada V, Boix RR, Horno M., "Resonant modes of circular microstrip patches in multilayered substrates", *IEEE Transactions on Microwave Theory and Techniques,* **47**(4), (1999), pp.488-498.

[2]- Losada V, Boix RR, Horno M., "Resonant modes of circular microstrip patches over ground planes with circular apertures in multilayered substrates containing anisotropic and ferrite materials", *IEEE Transactions on Microwave Theory and Techniques*, **48**(10), (2000), pp.1756-1762.

[3]- Kawano K, Tmimuro H., "Hybrid-mode analysis of a microstrip-slot resonator", *IEE proceedings,* **129**(6), (1982), pp.351-355.

[4]- Kawano K. Hybrid-mode analysis of coupled microstrip-slot resonators, *IEEE Transactions on Microwave Theory and Techniques,* **Mtt-33**(1), (1985), pp.38-43.

[5]- Bouttout F, Benabdelaziz F, Benghalia A, Khedrouche D, Fortaki T., "Uniaxially anisotropic substrate effects on resonance of rectangular microstrip patch antenna", *Electronics Letters,* **35**(4), (1999), pp.255-256.

[6]- Bouttout F, Benabdelaziz F, Fortaki T, Khedrouche D., "Resonant frequency and bandwidth of a superstrate-loaded rectangular patch on a uniaxial anisotropic substrate", *Communications in numerical methods in engineering,* **16**, (2000), pp.459-473.

[7]- Losada V, Boix R.R, Horno M., "Full-wave analysis of circular microstrip resonators in multilayered media containing uniaxial anisotropic dielectrics, magnetized ferrites, and chiral materials", *IEEE Transactions on Microwave Theory and Techniques,* **48**(6), (2000), pp.1057-1064.

[8]- Chew WC, Habashy T.M., "The use of vector transforms in solving some electromagnetic scattering problems", *IEEE Transactions on Antennas and Propagation*, **Ap-34**(7), (1986), pp.871-879.

[9]- Chew WC, Liu Q., "Resonance frequency of a rectangular microstrip patch. *IEEE Transactions on Antennas and Propagation* 1988; **36**(8):1045-1056.

[10]- Uwaro T, Itoh T. Spectral domain approach", In *Numerical techniques for microwave and millimeter-wave passive structures*, Itoh T (ed.); Wiley: New York, (1989), pp. 334-380.

[11]- Harrington RF., "Field Computation by Moment Method", Macmillan: New York, (1968).

[12]- Bouttout F, Benabdelaziz F, Khellaf A., "Closed-form Hankel transforms for circular disk basis modes involving Chebyshev polynomials and edge condition", *Electronics Letters,* **36**(10), (2000), pp.866-867.

[13]- Wong KL, Row JS, Kuo CW, Huang KC., "Resonance of a rectangular microstrip patch on a uniaxial substrate, *IEEE Transactions on Microwave Theory and Techniques,* **41**(4), (1993), pp.698-701.

[14]- Newman EH, Forrai D., "Scattering from a microstrip patch", *IEEE Transactions on Antennas and Propagation,* **Ap-35**(3), (1987), pp.245-251.

[15]- Popovic BD, Nesic A., "Some extensions of the concept of complementary electromagnetic structures", *IEE proceedings,* **132**(2), (1985), pp.131-137.

[16]- Aksun MI, Chuang SL, Lo YT., "On slot-coupled microstrip antennas and their applications to CP operation - theory and experiment", *IEEE Transactions on Antennas and Propagation,* **38**(8), (1990), pp.1224-1230. □